



A Hexanucleotide Repeat Expansion in *C9ORF72* Is the Cause of Chromosome 9p21-Linked ALS-FTD

Alan E. Renton, 1,38 Elisa Majounie, 2,38 Adrian Waite, 3,38 Javier Simón-Sánchez, 4,5,38 Sara Rollinson, 6,38 J. Raphael Gibbs, 7,8,38 Jennifer C. Schymick, 1,38 Hannu Laaksovirta, 9,38 John C. van Swieten, 4,5,38 Liisa Myllykangas, 10 Hannu Kalimo, 10 Anders Paetau, 10 Yevgeniya Abramzon, 1 Anne M. Remes, 11 Alice Kaganovich, 12 Sonja W. Scholz, 2,13,14 Jamie Duckworth, 7 Jinhui Ding, 7 Daniel W. Harmer, 15 Dena G. Hernandez, 2,8 Janel O. Johnson, 1,8 Kin Mok, 8 Mina Ryten, 8 Danyah Trabzuni, 8 Rita J. Guerreiro, 8 Richard W. Orrell, 16 James Neal, 17 Alex Murray, 18 Justin Pearson, 3 Iris E. Jansen, 4 David Sondervan, 4 Harro Seelaar, 5 Derek Blake, 3 Kate Young, 6 Nicola Halliwell, 6 Janis Bennion Callister, 6 Greg Toulson, 6 Anna Richardson, 19 Alex Gerhard, 19 Julie Snowden, 19 David Mann, 19 David Neary, 19 Michael A. Nalls, 2 Terhi Peuralinna, 9 Lilja Jansson, 9 Veli-Matti Isoviita, 9 Anna-Lotta Kaivorinne, 11 Maarit Hölttä-Vuori, 20 Elina Ikonen, 20 Raimo Sulkava, 21 Michael Benatar, 22 Joanne Wuu, 23 Adriano Chiò, 24 Gabriella Restagno, 25 Giuseppe Borghero, 26 Mario Sabatelli, 27 The ITALSGEN Consortium, 28 David Heckerman, 29 Ekaterina Rogaeva, 30 Lorne Zinman, 31 Jeffrey D. Rothstein, 14 Michael Sendtner, 32 Carsten Drepper, 32 Evan E. Eichler, 33 Can Alkan, 33 Ziedulla Abdullaev, 34 Svetlana D. Pack, 34 Amalia Dutra, 35 Evgenia Pak, 35 John Hardy, 8 Andrew Singleton, 2 Nigel M. Williams, 3,38 Peter Heutink, 4,38 Stuart Pickering-Brown, 6,38 Huw R. Morris, 3,36,37,38 Pentti J. Tienari, 9,38 and Bryan J. Traynor 1,14,38,*

¹Neuromuscular Diseases Research Unit, Laboratory of Neurogenetics, National Institute on Aging, National Institutes of Health, Bethesda, MD 20892, USA

²Molecular Genetics Unit, Laboratory of Neurogenetics, National Institute on Aging, National Institutes of Health, Bethesda, MD 20892, USA ³MRC Centre for Neuropsychiatric Genetics and Genomics, Cardiff University School of Medicine, Cardiff CF14 4XN, UK

⁴Department of Clinical Genetics, Section of Medical Genomics, and Alzheimer Disease Center, VU University Medical Centre, 1081 HV, Amsterdam, The Netherlands

⁵Department of Neurology, Erasmus MC - University Medical Center Rotterdam, 3015 CE, Rotterdam, The Netherlands

⁶Faculty of Human and Medical Sciences, University of Manchester, Manchester M13 9PT, UK

⁷Computational Biology Core, Laboratory of Neurogenetics, National Institute on Aging, National Institutes of Health, Bethesda, MD 20892, USA

⁸Department of Molecular Neuroscience and Reta Lila Weston Laboratories, Institute of Neurology, University College London, Queen Square House, London WC1N 3BG, UK

⁹Department of Neurology, Helsinki University Central Hospital and Molecular Neurology Programme, Biomedicum, University of Helsinki, Helsinki, FIN-02900, Finland

¹⁰Department of Pathology, Haartman Institute/HUSLAB, University of Helsinki and Folkhälsan Research Center (LM), Helsinki, FIN-02900. Finland

¹¹Institute of Clinical Medicine, Neurology, University of Oulu and Clinical Research Center, Oulu University Hospital, Oulu, FIN-90014, Finland
¹²Cell Biology and Gene Expression Unit, Laboratory of Neurogenetics, National Institute on Aging, National Institutes of Health, Bethesda, MD 20892, USA

¹³Department of Neuroscience, Georgetown University, Washington, D.C. 20057, USA

¹⁴Department of Neurology, Brain Sciences Institute, Johns Hopkins University, Baltimore, MD 21287, USA

¹⁵Illumina Inc., Hayward, CA 94545, USA

¹⁶Department of Clinical Neuroscience, Institute of Neurology, University College London, London NW3 2PG, UK

¹⁷Department of Pathology, Cardiff University School of Medicine, Cardiff CF14 4XN, UK

¹⁸Institute of Medical Genetics, University Hospital of Wales, Cardiff CF14 4XW, UK

¹⁹Neurodegeneration and Mental Health Research Group, Cerebral Function Unit, School of Community Based Medicine, University of Manchester, Manchester M6 8HD, UK

²⁰Institute of Biomedicine/Anatomy, University of Helsinki, Helsinki, FIN-00014, Finland

²¹Section of Geriatrics, Institute of Public Health and Clinical Nutrition, University of Eastern Finland, Kuopio, FIN-70211, Finland

²²Neuromuscular Division, Department of Neurology, University of Miami Miller School of Medicine, Miami, FL 33136, USA

²³Clinical Translational Research Division, Department of Neurology, University of Miami Miller School of Medicine, Miami, FL 33136, USA ²⁴Department of Neuroscience, University of Turin, 10126 Turin, Italy

²⁵Molecular Genetics Unit, Department of Clinical Pathology, A.S.O. O.I.R.M.-S. Anna, 10126 Turin, Italy

²⁶Department of Neurology, Azienda Universitaria-Ospedaliera di Cagliari and University of Cagliari, 09042 Cagliari, Italy

²⁷Neurological Institute, Catholic University and I.C.O.M.M. Association for ALS Research, 10100 Rome, Italy

²⁸For a list of consortium members, please see the Supplemental Information online

²⁹Microsoft Research, Los Angeles, CA 90024, USA

³⁰Tanz Centre for Research of Neurodegenerative Diseases and Toronto Western Hospital, Division of Neurology, Department of Medicine, University of Toronto, Toronto, ON, M5S 3H2, Canada

³¹Division of Neurology, Department of Internal Medicine, Sunnybrook Health Sciences Centre, University of Toronto, Toronto, ON, M4N 3M5, Canada

³²Institute for Clinical Neurobiology, University of Würzburg, D-97078 Würzburg, Germany

³³Howard Hughes Medical Institute and Department of Genome Sciences, University of Washington School of Medicine, Seattle, WA 98195. USA

³⁴Chromosome Pathology Unit, Laboratory of Pathology, National Cancer Institute, NIH, Bethesda, MD 20892, USA



- ³⁵Cytogenetics and Microscopy Core, National Human Genome Research Institute, National Institutes of Health, Bethesda, MD 20892, USA
- ³⁶Neurology (C4), University Hospital of Wales, Cardiff CF14 4XN, UK
- ³⁷Department of Neurology, Royal Gwent Hospital, Aneurin Bevan Local Health Board, Gwent NP20 2UB, UK
- ³⁸These authors contributed equally to this work

*Correspondence: traynorb@mail.nih.gov DOI 10.1016/j.neuron.2011.09.010

SUMMARY

The chromosome 9p21 amyotrophic lateral sclerosis-frontotemporal dementia (ALS-FTD) locus contains one of the last major unidentified autosomal-dominant genes underlying these common neurodegenerative diseases. We have previously shown that a founder haplotype, covering the MOBKL2b, IFNK, and C9ORF72 genes, is present in the majority of cases linked to this region. Here we show that there is a large hexanucleotide (GGGGCC) repeat expansion in the first intron of C9ORF72 on the affected haplotype. This repeat expansion segregates perfectly with disease in the Finnish population, underlying 46.0% of familial ALS and 21.1% of sporadic ALS in that population. Taken together with the D90A SOD1 mutation, 87% of familial ALS in Finland is now explained by a simple monogenic cause. The repeat expansion is also present in onethird of familial ALS cases of outbred European descent, making it the most common genetic cause of these fatal neurodegenerative diseases identified to date.

INTRODUCTION

Amyotrophic lateral sclerosis (ALS, OMIM #105400) is a fatal neurodegenerative disease characterized clinically by progressive paralysis leading to death from respiratory failure, typically within two to three years of symptom onset (Rowland and Shneider, 2001). ALS is the third most common neurodegenerative disease in the Western world (Hirtz et al., 2007), and there are currently no effective therapies. Approximately 5% of cases are familial in nature, whereas the bulk of patients diagnosed with the disease are classified as sporadic as they appear to occur randomly throughout the population (Chiò et al., 2008). There is growing recognition, based on clinical, genetic, and epidemiological data, that ALS and frontotemporal dementia (FTD, OMIM #600274) represent an overlapping continuum of disease, characterized pathologically by the presence of TDP-43 positive inclusions throughout the central nervous system (Lillo and Hodges, 2009; Neumann et al., 2006).

To date, a number of genes have been discovered as causative for classical familial ALS, namely SOD1, TARDBP, FUS, OPTN, and VCP (Johnson et al., 2010; Kwiatkowski et al., 2009; Maruyama et al., 2010; Rosen et al., 1993; Sreedharan et al., 2008; Vance et al., 2009). These genes cumulatively account for \sim 25% of familial cases, indicating that other causa-

tive genes remain to be identified. Each new gene implicated in the etiology of ALS or FTD provides fundamental insights into the cellular mechanisms underlying neuron degeneration, as well as facilitating disease modeling and the design and testing of targeted therapeutics; thus, the identification of new genes that cause ALS or FTD is of great significance.

Linkage analysis of kindreds involving multiple cases of ALS, FTD, and ALS-FTD had suggested that there was an important locus for the disease on the short arm of chromosome 9 (Boxer et al., 2011; Morita et al., 2006; Pearson et al., 2011; Vance et al., 2006). Using a genome-wide association study (GWAS) approach, we recently reported that this locus on chromosome 9p21 accounted for nearly half of familial ALS and nearly onequarter of all ALS cases in a cohort of 405 Finnish patients and 497 control samples (Laaksovirta et al., 2010). This association signal had previously been reported by van Es and colleagues (van Es et al., 2009), and a meta-analysis involving 4,312 cases and 8,425 controls confirmed that chromosome 9p21 was the major signal for ALS (Shatunov et al., 2010). A recent GWAS for FTD also identified this locus (Van Deerlin et al., 2010). Analysis in the Finnish population narrowed the association to a 232 kilobase (kb) block of linkage disequilibrium and allowed the identification of a founder haplotype that increased risk of disease by over 20-fold. The associated haplotype appears to be the same in all European-ancestry populations, and several families previously shown to have genetic linkage to the chromosome 9p21 region also share this risk haplotype (Mok et al., 2011).

We have previously identified an ALS-FTD family from the UK and an apparently unrelated ALS-FTD family from the Netherlands that showed positive linkage to the chromosome 9p21 region (Mok et al., 2011; Pearson et al., 2011). Using these families and the Finnish ALS cases that had previously been used to identify the chromosome 9p21 association signal, we undertook a methodical assessment of the region using next-generation sequencing technology in an attempt to identify the genetic lesion responsible for disease.

RESULTS

We undertook massively parallel, next-generation, deep resequencing of the chromosome 9p21 region in (1) DNA that had been flow-sorted enriched for chromosome 9 obtained from an affected member of the GWENT#1 kindred (IV-3, Figure 1A; Coriell ID ND06769) and from a neurologically normal control (ND11463); and (2) DNA that had been enriched for the target region using custom oligonucleotide baits obtained from three cases and five unaffected members of the DUTCH#1 kindred (V-1, V-3, and V-14, and V-2, V4, V5, VI-1, and spouse of V-1; Figure 1B).



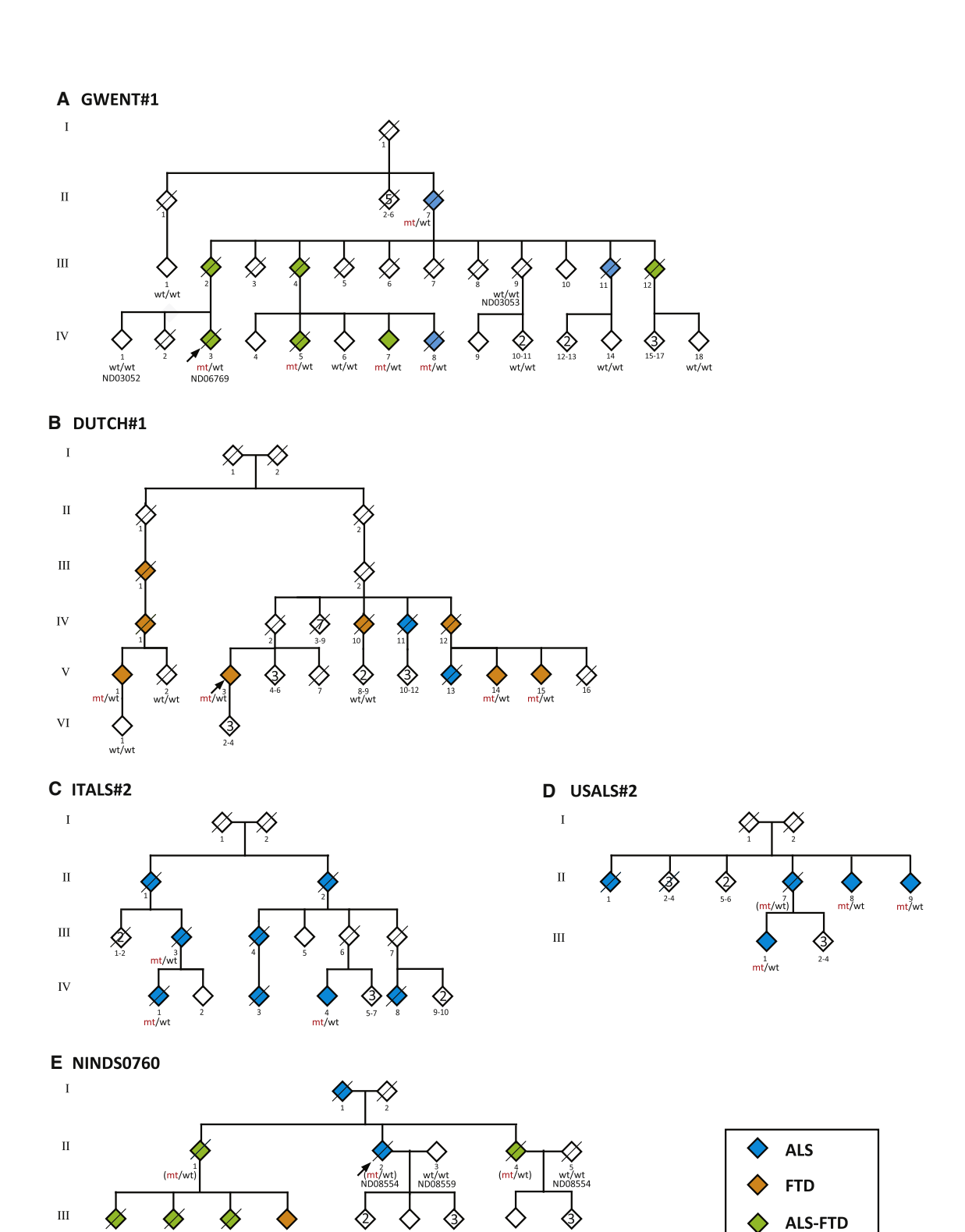
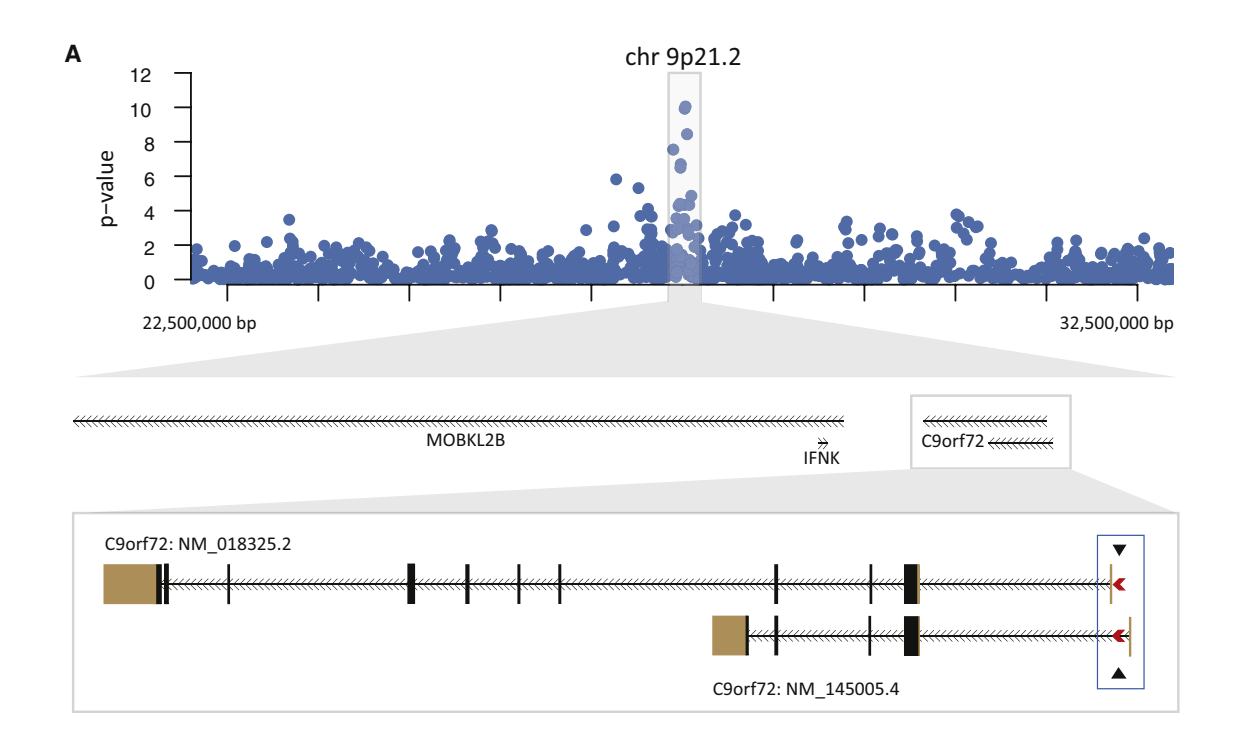


Figure 1. Pedigrees of Patients Carrying the C90RF72 GGGGCC Hexanucleotide Repeat Expansion

(A-E) Pedigrees of patients with the hexanucleotide repeat expansion. Mutant alleles are shown by mt, whereas wild-type alleles are indicated by wt. Inferred genotypes are in brackets. Blue diamonds represent a diagnosis of ALS, orange diamonds represent FTD, and green diamonds represent ALS-FTD. Probands are indicated by arrows. Sex of the pedigree members is obscured to protect privacy.





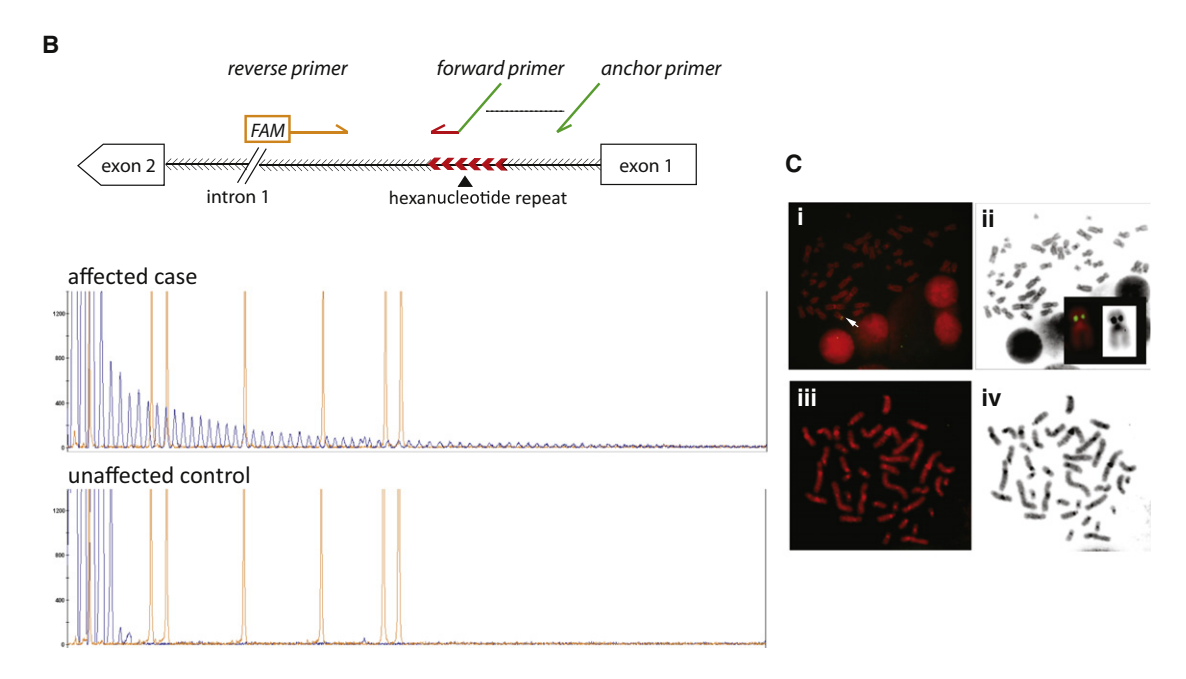


Figure 2. GGGGCC Hexanucleotide Repeat Expansion in the First Intron and Promoter of C90RF72

(A) Physical map of the chromosome 9p21 ALS/FTD locus showing the p values for SNPs genotyped in the previous GWAS (Laaksovirta et al., 2010), the location of the GWAS association signal within a 232 kb block of linkage disequilibrium, the *MOBKL2B*, *IFNK*, and *C9ORF72* genes within this region, and the position of the GGGGCC hexanucleotide repeat expansion within the two main transcripts of *C9ORF72* (RefSeq accession numbers NM_018325.2 and NM_145005.4, see online http://www.ncbi.nlm.nih.gov/RefSeq/ for further details; GenBank accession numbers GI:209863035 and GI:209863036, see online http://www.ncbi.nlm.nih.gov/genbank/ for further details).

(B) A graphical representation of primer binding for repeat-primed PCR analysis is shown in the upper panel. In the lower panel, capillary-based sequence traces of the repeat-primed PCR are shown. Orange lines indicate the size markers, and the vertical axis represents fluorescence intensity. A typical saw tooth tail pattern that extends beyond the 300 bp marker with a 6 bp periodicity is observed in the case carrying the GGGGCC repeat expansion.

(C) Detection of the repeat expansion in the lymphoblastoid cell line from the affected proband of the GWENT#1 kindred (ND06769) by FISH using Alexa Fluor 488-labeled oligonucleotide probe seen as a green fluorescence signal on one of the homologs of chromosome 9p (i) consistent with a repeat expansion size of



Analysis of the GWENT#1 sequence data revealed eight novel variants within the 232 kb block of linkage disequilibrium containing the previously identified association signal that were not described as polymorphisms in either the 1000 Genomes (April 2009 release) or the dbSNP (build 132) online databases. Six of these variants were located within a 30 base pair (bp) region. When the individual sequence reads within this region were examined and manually realigned, they indicated the presence of a hexanucleotide repeat expansion GGGGCC located 63 bp centromeric to the first exon of the long transcript of C9ORF72 (RefSeq accession number = NM_018325.2; GenBank accession number = GI:209863035) in the affected cases that was not present in the control samples (see Figure S1 available online for individual reads). The repeat expansion also lies within the first intron of the other major transcript of C9ORF72 (RefSeg accession number = NM_145005.4; GenBank accession number = GI:209863036; Figure 2A).

We next used a repeat-primed PCR method to screen case and control samples for the presence of the GGGGCC hexanucleotide repeat expansion (see Figure 2B and Experimental Procedures for a detailed explanation) (Kobayashi et al., 2011; Warner et al., 1996). The nature of the repeat-primed PCR assay means that it can detect a maximum of ~60 repeats, and thus the repeat length in a sample carrying the expansion could be far greater than the estimation provided by this technique. Despite this, the assay is an accurate and rapid system that allows samples to be categorized into those that carry a pathogenic repeat expansion (greater than 30 repeats) and those that carry only wild-type alleles (fewer than 20 repeats). The frequency distribution of the GGGGCC hexanucleotide repeat expansion lengths in ALS cases and control samples based on the repeat-primed PCR assay is shown in Figure 3.

Using the repeat-primed PCR method, we confirmed that the expanded hexanucleotide repeat was present in the affected members of the GWENT#1 and DUTCH#1 kindreds (IV-3, IV-5, IV-7, and IV-8 in GWENT#1 and V-1, V-3, V-14, V-15 in DUTCH#1, Figures 1A and 1B) and that the expansion was absent from asymptomatic family members (III-1, III-9, IV-1 in GWENT#1 and V-2, V-8, V-9, and VI-1 in DUTCH#1).

In the Finnish cohort of 402 ALS cases and 478 controls, repeat-primed PCR analysis showed the hexanucleotide repeat to be expanded in 113 (28.1%) cases and 2 (0.4%) controls (Fisher's exact test p value for allelic association = 8.1 \times 10 $^{-38}$; OR = 78.0, 95% CI = 19.2–316.8). Overall, 52 (46.4%) of the Finnish familial ALS cases had the expansion (p value = 3.7 \times 10 $^{-37}$; OR = 140.9, 95% CI = 34.0–583.9), and 61 (21.0%) of the sporadic cases had the expansion (p value = 1.7 \times 10 $^{-24}$; OR = 56.1, 95% CI 13.6–230.2). The average number of repeats detected by the PCR assay in the Finnish cases carrying the expansion was 53 (range, 30 to 71) compared to an average of 2 (range, 0 to 22) repeats observed in the 476 controls that did not carry the expansion, thereby allowing for robust classification of samples (see Figures 3A and 3B).

Of the 113 familial and sporadic Finnish cases that carried the hexanucleotide repeat expansion, two-thirds (n = 76, 67.3%) carried the previously identified chromosome 9p21 founder risk haplotype (Laaksovirta et al., 2010). In contrast, only one of the Finnish controls samples that carried the expansion also carried the risk haplotype.

For confirmation of the repeat expansion and to estimate its size, fluorescence in situ hybridization (FISH) was performed in an affected member of the GWENT#1 kindred (IV-3, Figure 1A, ND06769), in a case from the NINDS0760 pedigree (III-1, Figure 1E), and in neurologically normal controls (ND11463, ND08559, ND03052, and ND03053). These experiments used a fluorescently labeled oligonucleotide probe consisting of three GGGGCC repeats (Haaf et al., 1996). All metaphases of the cases showed a strong hybridization signal to a single chromosome-9p21-consisting of a discrete dot on each sister chromatid (Figure 2C). Fluorescence was not detected in any metaphases of the control samples. These experiments indicated that the expansion was at least 1.5 kb (representing \sim 250 GGGCC repeats) in size, which is the minimum detectable size of a repeat using this technique (Liehr, 2009). Additional experimental approaches, such as Southern blotting, will be needed to determine the true repeat length with greater precision.

Our data clearly showed the importance of the hexanucleotide repeat expansion within the Finnish ALS population and in families linked to the chromosome 9p21 region. To further determine the frequency of the hexanucleotide expansion in outbred European populations, we screened a cohort of 268 familial ALS probands from North America (n = 198), Germany (n = 41), and Italy (n = 29) using repeat-primed PCR. Of these cases, 102 (38.1%) carried the same hexanucleotide GGGCC repeat expansion within C9ORF72 (Figure 3C). Within this dataset, we identified three additional multigenerational families where the presence of the repeat expansion segregated perfectly with disease within the kindred (Figures 1C-1E). In contrast, the repeat expansion was not detected in 262 U.S. Caucasian controls, 83 Italian controls, and 64 German controls (total number of control chromosomes = 818, average number of repeats = 3, range 0-18, Figure 3D). An additional series of 300 anonymous African and Asian samples that are part of the Human Gene Diversity Panel (Cann et al., 2002) were included in the mutational analysis as controls to evaluate the genetic variability of the C9ORF72 hexanucleotide repeat expansion in non-Caucasian populations. None of these samples carried more than 15 GGGGCC repeats (average number of repeats = 3, range = 0-15).

Given the genetic and clinical overlap between ALS and FTD, as well as the co-occurrence of ALS and FTD within families linked to the chromosome 9p21 locus, we tested the hypothesis that the hexanucleotide repeat expansion may underlie a proportion of FTD cases by measuring its occurrence in a cohort of 75 Finnish FTD cases using the same repeat-primed PCR method.

more than 1.5 kb. DAPI-inverted image (ii and iv). No hybridization signal was detected on metaphase cells or interphase nuclei from the lymphoblastoid cell line of control individual ND 11463 (iii) and five other normal control individuals (data not shown). Cells were counterstained with 4′,6-diamidino-2-phenylindole (DAPI, red color), 60× objective.



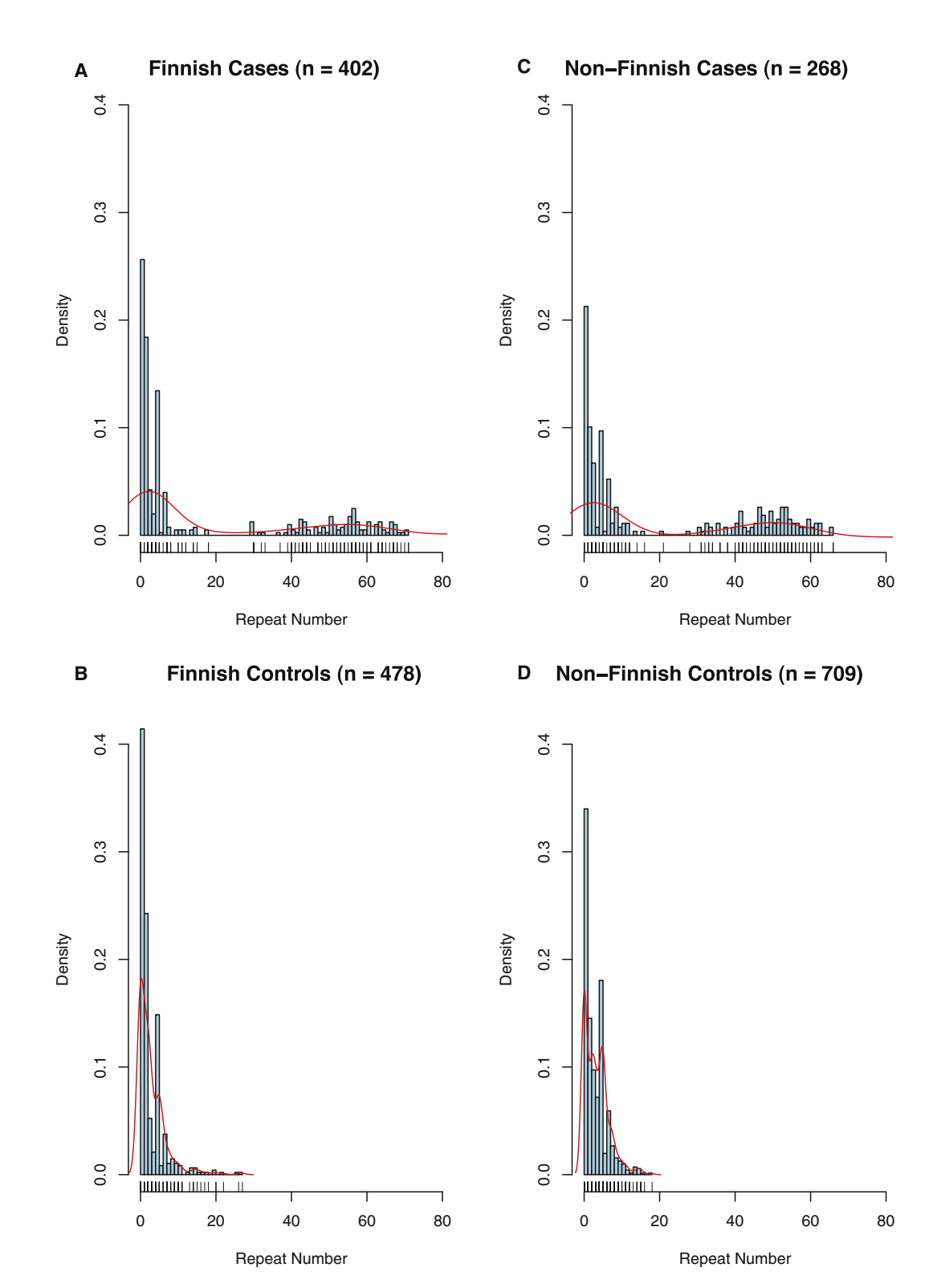
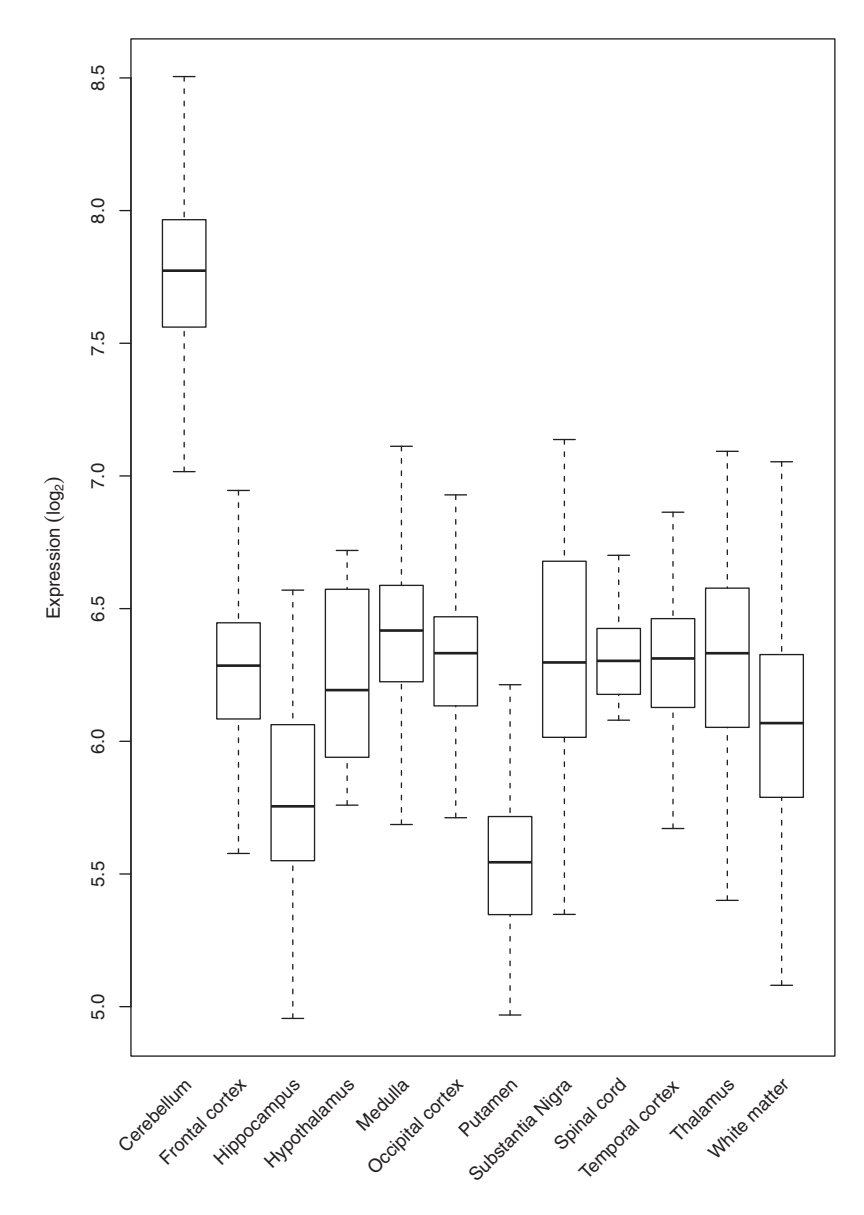


Figure 3. Repeat-Primed PCR Assay Distinguishes Samples Carrying a Pathogenic GGGGCC Hexanucleotide Repeat Expansion in the C90RF72 Gene from Wild-Type Samples

A bimodal distribution is evident with samples carrying the repeat expansion showing 30 or more repeats and control samples having fewer than 20 repeats. The repeat-primed PCR assay determines whether or not a sample carries a large pathogenic expansion but does not measure the actual number of repeats in a large pathogenic expansion.

(A) Histogram of repeat lengths based on the repeat-primed PCR assay observed in Finnish cases (n = 402).





The percentage of these FTD cases carrying the repeat expansion was comparable to that of the Finnish ALS cohort (n = 22, representing 29.3% of the cohort), and the GGGGCC repeat expansion was highly associated with FTD in the Finnish population (Fisher's exact test p value based on 75 Finnish FTD cases and 478 Finnish controls = 4.3×10^{-18} ; OR = 82.0, 95% CI 19.1-352.8). Six of the Finnish FTD cases carrying the repeat expansion presented with progressive nonfluent aphasia, and the remaining 16 patients had clinical features consistent with behavioral-variant FTD. In addition, 8 (36.4%) of these Finnish FTD patients had a personal or family history of ALS.

Figure 4. Expression Analysis of C9ORF72 RNA

Expression array analysis of C9ORF72 in various human CNS regions obtained from neuropathologically normal individuals (n = 137).

Using expression arrays, C9ORF72 RNA was detected across multiple CNS tissues obtained from neuropathologically normal individuals including spinal cord, with the highest expression level observed within the cerebellum (Figure 4). Real-time RT-PCR analysis of expression in frontal cortex tissue obtained from patients and controls did not find any conclusive change in RNA levels and produced inconsistent results across different labs and different samples (see Figure S2 available online for preliminary data).

Immunocytochemistry using an antibody that recognizes both human and mouse C9ORF72 (Santa Cruz Biotechnology) found the protein to be predominantly localized within the nucleus in human control fibroblast cell lines and in the mouse motor neuron NSC-34 cell line (Figure 5). Furthermore, C9ORF72 protein levels appeared to be reduced in fibroblast cell lines derived from ALS patients relative to controls, with relatively more cytoplasmic staining in cases compared to controls. However, these data must be considered to be preliminary, as firm conclusions cannot be drawn based on a small number of samples. Furthermore, the Santa Cruz C9ORF72 antibody used for these experiments is largely uncharacterized: preliminary data suggest that siRNA knockdown of C9ORF72 mRNA results in a mild reduction of C9ORF72 protein by western blot in H4 and T98G cells, though a similar effect was also seen using siRNA allstar control (see Figure S3 online). At this stage, the question of whether the pathogenic expansion is associated with a decrease

in protein expression remains unresolved. Future experiments requiring generation of more specific antibodies and more quantitative approaches will be needed to definitively determine the localization of the different C9ORF72 isoforms in different tissues and at various stages of disease progression.

DISCUSSION

In this paper, we used next-generation sequencing technology to identify a hexanucleotide repeat expansion within the C9ORF72 gene as the cause of chromosome 9p21-linked

⁽B) Histogram of repeat lengths based on the repeat-primed PCR assay observed in Finnish controls (n = 478).

⁽C) Histogram of repeat lengths based on the repeat-primed PCR assay in familial ALS cases of general European (non-Finnish) descent (n = 268).

⁽D) Histogram of repeat lengths based on the repeat-primed PCR assay in control samples of European descent (n = 409) and Human Gene Diversity Panel samples (n = 300).



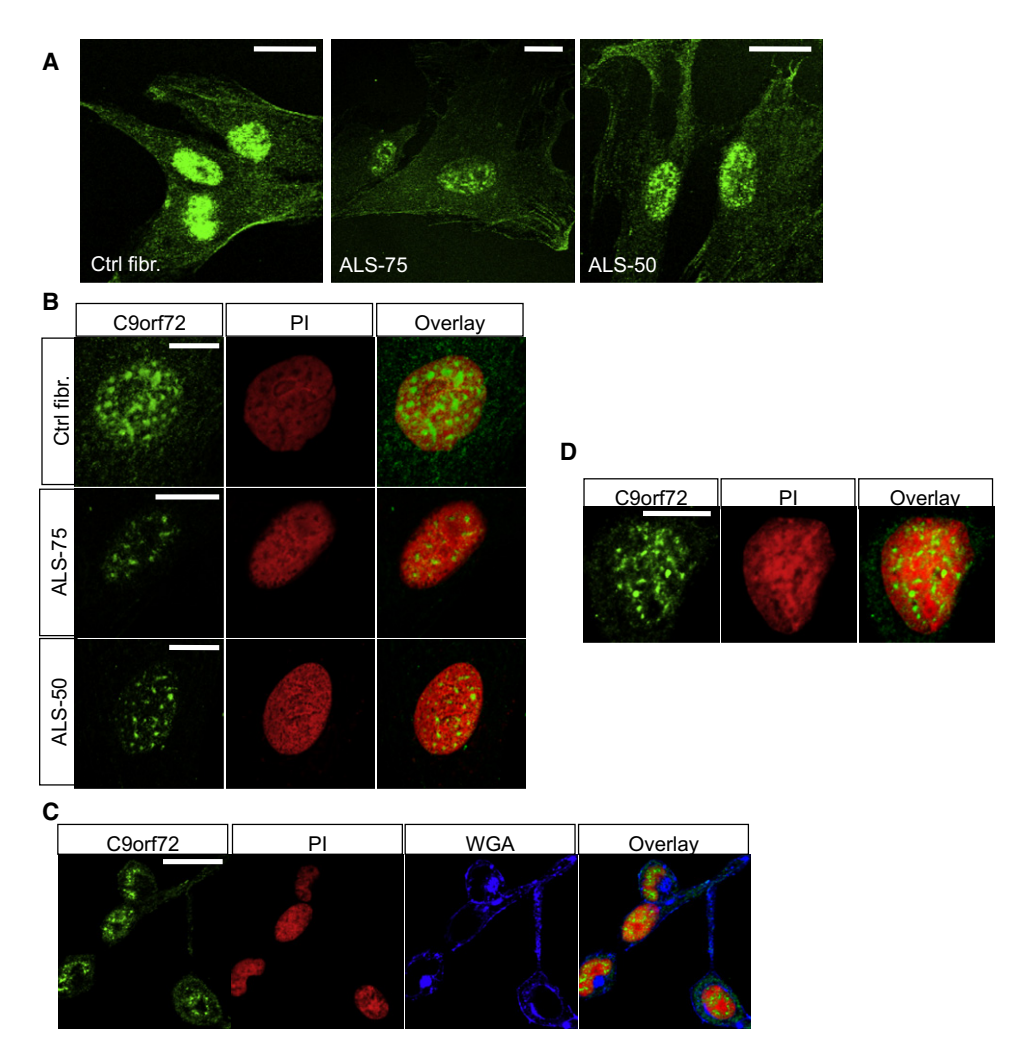


Figure 5. Preliminary Analysis of C9ORF72 Protein Levels in Control Cell Lines and Cell Lines Derived from ALS Patients

(A) Immunocytochemistry of C9ORF72 protein in human-derived primary fibroblasts obtained from a healthy individual (Ctrl fibr.) and from ALS patients (ALS-75 and ALS-50). Green signals represent C9ORF72 (Santa Cruz antibody). Scale bars represent 20 µm.

(B) Nuclear staining pattern of C9ORF72 protein in control and ALS fibroblasts. Green signals represent C9ORF72 protein (Santa Cruz) and red signals represent propidium iodide (PI) (nuclear stain). Scale bars represent 20 μm.

(C) Immunocytochemistry of C9ORF72 protein in mouse-derived NSC-34 motor neuron cell line. Green signals represent C9ORF72 protein (Santa Cruz), red signals represent propidium iodide (PI) (nuclear stain), and blue signals represent wheat germ agglutinin (WGA) (membrane stain). Scale bar represents 20 μm. (D) Nuclear staining pattern of C9ORF72 protein in NSC-34 mouse motor neuron cell line. Green signals represent C9ORF72 protein, and red signals represent propidium iodide (PI) (nuclear stain). Scale bars represent 20 μm.

ALS-FTD and subsequently confirmed the presence of this large expansion in a substantial proportion of familial ALS and FTD cases. Overall, the hexanucleotide repeat expansion was found in nearly one-half of Finnish familial ALS cases and in more than one-third of familial ALS cases of wider European ancestry. Our data indicate that the repeat expansion is more than twice as common as mutations in the *SOD1* gene as a cause of familial ALS (Chiò et al., 2008) and more than three times as common as *TARDBP*, *FUS*, *OPTN*, and *VCP* mutations combined (Johnson et al., 2010; Mackenzie et al., 2010; Maruyama et al., 2010). Taken together with the D90A *SOD1* mutation, our data show that nearly 90% of familial ALS in Finland is now explained by a simple monogenic cause.

We present five pieces of genetic data demonstrating that the hexanucleotide repeat expansion is pathogenic for neurodegeneration. First, the hexanucleotide expansion segregated with disease within two multigenerational kindreds that have been convincingly linked to the region (Pearson et al., 2011). Second, the hexanucleotide expansion was highly associated with disease in the same cohort of ALS cases and controls that was used to identify the chromosome 9p21 region within the Finnish population. Furthermore, the association signal based on the presence or absence of the expansion was many times greater than that indicated by the surrounding SNPs (p value based on expansion = 8.1×10^{-38} versus 9.11×10^{-11} based on the most associated SNP rs3849942 in the initial Finnish ALS



GWAS) (Laaksovirta et al., 2010). Third, the hexanucleotide repeat expansion was not found in 409 population-matched control subjects or in 300 diverse population samples screened in our laboratory. Fourth, we found that a large proportion of apparently unrelated familial ALS and FTD cases carried the same hexanucleotide repeat expansion within C9ORF72. Within this cohort of European-ancestry familial samples, we identified three additional multigenerational families within which the repeat expansion segregated perfectly with disease. Fifth, FISH analysis demonstrated that the repeat expansion is large in size (at least 1.5 kb to be visualized by this technique, Figure 2C), and such long expansions are typically pathogenic (Kobayashi et al., 2011). Finally, another group independently discovered the same genetic mutation to be the cause of chromosome 9p21-linked FTD/ALS (DeJesus-Hernandez et al., 2011).

Our data indicate that both ALS and FTD phenotypes are associated with the *C9ORF72* GGGGCC hexanucleotide repeat expansion. Several members of the GWENT#1 and DUTCH#1 pedigrees manifested clinical signs of isolated motor neuron dysfunction or isolated cognitive decline, whereas other affected members developed mixed ALS-FTD symptomatology over the course of their illness (Pearson et al., 2011). It is interesting to note that the frequency of the repeat expansion was almost identical in our ALS and FTD case cohorts, suggesting that carriers of the mutant allele are equally at risk for both forms of neurodegeneration. Our data support the notion that the observed clinical and pathological overlap between ALS and FTD forms of neurodegeneration may be driven in large part by the *C9ORF72* hexanucleotide repeat expansion.

The identification of the cause of chromosome 9p21-linked neurodegeneration allows for future screening of populationbased cohorts to further unravel the overlap between ALS and FTD and to identify additional genetic and environmental factors that push an individual's symptoms toward one end of the ALS/FTD clinical spectrum. Some early observations may already be made: among our Finnish FTD cohort, we identified several patients carrying the pathogenic repeat expansion who presented with nonfluent progressive aphasia. This suggests that the difficulties with speech production that are commonly observed in ALS patients may in some cases be partially attributable to cortical degeneration in addition to tongue and bulbar musculature weakness secondary to hypoglossal motor neuron degeneration. It is also interesting to note that age of symptom onset varied widely in patients carrying the pathogenic hexanucleotide expansion, including some individuals who developed weakness in their ninth decade of life. The genetic and/or environmental factors underlying this variability remain to be determined.

Our development of a rapid, reliable method of screening individuals for the repeat expansion will have immediate clinical utility by allowing early identification of ALS patients at increased risk of cognitive impairment, and of FTD cases at increased risk of progressive paralysis. In the longer term, the identification of the genetic lesion underlying chromosome 9p21-linked ALS and FTD, together with the observed high frequency in these patient populations, makes it an ideal target for drug development aimed at amelioration of the disease process.

Broadly speaking, pathogenic repeat expansions are thought to cause disease through haploinsufficiency, in which expression or splicing of the target gene is perturbed, or through the generation of abnormal amounts of toxic RNA that disrupt normal cellular pathways. We favor the second as a mechanism in chromosome 9 FTD/ALS, given the large size of the expansion visualized by FISH and its noncoding localization within the C90RF72 gene. RNA generated from such pathogenic repeat expansions are thought to disrupt transcription by sequestering normal RNA and proteins involved in transcription regulation (Wojciechowska and Krzyzosiak, 2011), and disruption of RNA metabolism has already been implicated in the pathogenesis of ALS associated with mutations in TDP-43 and FUS (Lagier-Tourenne et al., 2010). Interestingly, an index family studied previously demonstrating aberrant RNA metabolism of an astroglial gene, EAAT2, (Lin et al., 1998) is in fact a chromosome 9 hexanucloitude mutation carrier. This might provide early evidence that aberrant RNA metabolism occurs as part of the pathogenic mechanism. However, knowing the pattern of distribution of C9ORF72 expression is likely to be key in understanding cell vulnerability and local expression of the hexanucleotide repeat expansion, which is probably influenced by the promoter of the C9ORF72 gene. We did not find consistent differences in expression between cases and controls. This may represent the true biological effect of the GGGGCC hexanucleotide repeat expansion on C9ORF72 expression, or alternatively it may reflect the small number of samples analyzed or tissue-to-tissue variation in expression of this gene. More definitive experimental testing is required in the future to resolve the effect of the hexanucleotide repeat expansion on C9ORF72 expression, as well as additional molecular biology investigation to understand the precise mechanism by which the hexanucleotide repeat may disrupt RNA metabolism.

An important aspect of understanding a pathogenic repeat expansion focuses on its stability. Preliminary evidence suggests that the C9ORF72 hexanucleotide repeat expansion may be unstable. First, minor anticipation has been noted in pedigrees that originally identified the locus with earlier generations being relatively unaffected by disease, perhaps reflecting expanding repeat number over successive generations (Vance et al., 2006). Interestingly, anticipation was not observed within the five families in which we found the hexanucleotide repeat expansion (see Figure 1). Second, although there was strong concordance between the presence of the chromosome 9p21 founder risk haplotype and the presence of the hexanucleotide expansion in an individual, the expansion was also present in ALS cases that did not carry this haplotype. These data are consistent with the expansion occurring on multiple occasions on multiple haplotype backgrounds. Taken together, these observations suggest that the C9ORF72 repeat region has some degree of instability. This instability may be particularly relevant for sporadic ALS, where the apparent random nature of the disease in the community could be a consequence of stochastic expansion in the number of repeats. It is noteworthy that a sizeable proportion of the Finnish ALS cases that carried the repeat expansion was clinically classified as sporadic.

In summary, our data demonstrate that a massive hexanucleotide repeat expansion within C9ORF72 is the cause of



Table 1. Demographic and Clinical Details of ALS Cases, FTD Cases, and Neurologically Normal Controls According to Geographical Region of Origin and GGGGCC Hexanucleotide Repeat Expansion Carrier Status

	European-Descent Familial ALS Case (n = 268) ^a	European-Descent Controls (n = 409) ^b	Finnish FTD Cases (n = 75)	Finnish ALS Cases (n = 402) ^c	Finnish Controls (n = 478) ^d	ALS Cases with Expansion (n = 215) ^e
Mean age (range)	56.5 (15–90)	44.1 (4–91)	58.4 (38-79)	56.8 (18–85)	88.6 (85–101)	56.6 (35–80)
Male (%)	144 (53.7%)	165 (40.4%)	34 (45.3%)	199 (49.5%)	96 (20.1%)	112 (52.1%)
Familial (%)	268 (100%)	-	27 (36.0%)	112 (27.9%)	-	154 (71.6%)
Site of Symptom Onset				,	·	
Bulbar-onset (%)	53 (26.4%)	-	-	94 (27.8%)	-	58 (32.6%)
Spinal-onset (%)	148 (73.6%)	-	-	244 (72.2%)	-	120 (67.4%)
Behavior variant FTD (%)	-	-	48 (64.0%)	-	-	-
Progressive nonfluent aphasia (%)	-	-	20 (26.7%)	-	-	-
Semantic dementia (%)	-	-	7 (9.3%)	-	-	-

Mean age represents age at symptom onset for cases and age at sample collection for controls.

chromosome 9p21-linked ALS, FTD, and ALS-FTD. Furthermore, this expansion accounts for an unprecedented proportion of ALS cases in Finland and in familial ALS cases of European ancestry, and it provides additional evidence supporting the role of disrupted RNA metabolism as a cause of neurodegeneration.

EXPERIMENTAL PROCEDURES

Patients and Material

We studied a four-generation Welsh family (GWENT#1) in which 9 individuals had been diagnosed with ALS and/or FTD and were known to share the chromosome 9p21 risk haplotype. The pedigree of this family is shown in Figure 1A, and the clinical features have been previously reported (Pearson et al., 2011). DNA samples were available from four individuals of generation IV who had been diagnosed with ALS and/or FTD. Flow-sorting of chromosome 9 was performed on lymphoblastoid cell lines from an affected case ND06769 (IV-3, Figure 1A) and a neurologically normal population control ND11463 at Chrombios GmbH (http://www.chrombios.com) using a FACS Vantage cell sorter (BD Biosciences, Franklin Lakes, NJ, USA).

We also analyzed an apparently unrelated six-generation Dutch ALS/FTD family (DUTCH#1, Figure 1B), in which linkage and haplotype analysis showed significant linkage to a 61 Mb region on chromosome 9p21 spanning from rs10732345 to rs7035160 and containing 524 genes and predicted transcripts. Genomic regions from all exons and exon-intron boundaries, 5′ UTRs, 3′ UTRs, ~650 bp of upstream promoter regions, sno/miRNA loci, and conserved regions were captured using SureSelect target enrichment technology (Agilent, Santa Clara CA, USA). In total, 43,142 unique baits were used for these experiments covering a total of 2.58 MB in the chromosome 9p FTD/ALS locus (c9FTD/ALS).

For subsequent mutational screening of the GGGGCC hexanucleotide repeat expansion, we used DNA from 402 Finnish ALS cases and 478 Finnish neurologically normal individuals that had previously been used to identify the chromosome 9p21 association signal (Laaksovirta et al., 2010). An additional 268 DNA samples were obtained from affected probands in unrelated ALS families (198 U.S. cases, 41 German cases, and 29 Italian cases) and from 75 Finnish individuals who had presented with isolated FTD. Control samples consisted of 262 neurologically normal US individuals obtained from the

NINDS repository at Coriell, 64 neurologically normal German individuals, and 83 neurologically normal Italian individuals. An additional series of 300 anonymous African and Asian samples that are part of the Human Gene Diversity Panel (Cann et al., 2002) were included in the mutational analysis as controls to evaluate the genetic variability of the repeat expansion in non-Caucasian populations. Demographics and clinical features of these samples are summarized in Table 1. Appropriate institutional review boards approved the study.

Next-Generation Sequencing

Paired-end sequencing was performed on a next-generation HiSeq2000 sequencer according to the manufacturer's protocol (Illumina, San Diego, CA, USA). This generated 56.7 gigabases of alignable sequence data for the control sample ND11463 (mean read depth for the chromosome 9 region 27,367,278 to 27,599,746 bp = 42.2) and 114.4 gigabases for the case sample ND06769 (mean read depth = 170.4). Sequence alignment and variant calling were performed against the reference human genome (UCSC hg 18). Sequencing reads were aligned using BWA (Li and Durbin, 2009). Sorting, indexing, read duplicate removal, and merging of BAM files were preformed with Picard (http://picard.sourceforge.net). The Genome Analysis Toolkit was used to perform base quality score recalibration and to call variants (McKenna et al., 2010). SNPs identified within CEU individuals from the 1000 Genomes project (April 2009 release, http://www.1000genomes.org) or in dbSNP (http://www.ncbi.nlm.nih.gov/projects/SNP/, Build 132) were excluded. The remaining variants were annotated to RefSeg transcripts and protein coding variants prioritized for examination.

Repeat-Primed PCR

Repeat-primed PCR was performed as follows: 100 ng of genomic DNA were used as template in a final volume of 28 μl containing 14 μl of FastStart PCR Master Mix (Roche Applied Science, Indianapolis, IN, USA), and a final concentration of 0.18 mM 7-deaza-dGTP (New England Biolabs, Ipswich, MA, USA), 1× Q-Solution (QIAGEN, Valencia, CA, USA), 7% DMSO (Sigma-Aldrich), 0.9 mM MgCl₂ (QIAGEN), 0.7 μM reverse primer consisting of \sim four GGGGCC repeats with an anchor tail, 1.4 μM 6FAM-fluorescent labeled forward primer located 280 bp telomeric to the repeat sequence, and 1.4 μM anchor primer corresponding to the anchor tail of the reverse primer (sequences available online in Supplemental Experimental Procedures) (Kobayashi et al., 2011; Warner et al., 1996). A touchdown PCR cycling

^a Data missing for age at onset (n = 12), and site of onset (n = 67).

^bData missing for age at sampling (n = 1) and gender (n = 1).

^c Data missing for age at onset (n = 29), site of onset (n = 64) and familial status (n = 1).

^d Data missing for age at collection (n = 6).

^e Data missing for age at onset (n = 18) and site of onset (n = 37).



program was used where the annealing temperature was gradually lowered from 70°C to 56°C in 2°C increments with a 3 min extension time for each cycle.

The repeat-primed PCR is designed so that the reverse primer binds at different points within the repeat expansion to produce multiple amplicons of incrementally larger size. The lower concentration of this primer in the reaction means that it is exhausted during the initial PCR cycles, after which the anchor primer is preferentially used as the reverse primer. Fragment length analysis was performed on an ABI 3730xl genetic analyzer (Applied Biosystems, Foster City, CA, USA), and data were analyzed using GeneScan software (version 4, ABI). Repeat expansions produce a characteristic sawtooth pattern with a 6 bp periodicity (Figure 2B).

Statistical Analysis

Our previous GWAS data suggested no significant population stratification within the Finnish population (Laaksovirta et al., 2010). Therefore, association testing was performed using the Fisher's exact test as implemented within the PLINK software toolkit (version 1.7) (Purcell et al., 2007).

FISH Analysis

Metaphase and interphase FISH analysis of lymphoblastoid cell lines ND06769 (case IV-3 from GWENT#1, Figure 1A), ND08554 (case II-2 from NINDS0760, Figure 1E), ND11463 (control), ND11417 (control), ND08559 (unaffected spouse II-3 from NINDS0760), ND03052 (unaffected relative IV-1 from GWENT#1), and ND03053 (unaffected relative III-9 from GWENT#1), as well as a fibroblast cell line (Finnish sample ALS50), was performed using Alexa fluor 488-labeled GGCCCGGCCCCGGCC oligonucleotide probe (Eurofins MWG operon, Hunstville, AL, USA) designed against the repeat expansion. The hybridization was performed in low-stringency conditions with 50% Formamide/2xSSC/10% Dextran Sulfate codenaturation of the slide/probe, 1 hr hybridization at 37°C, followed by a 2 min wash in 0.4×SSC/0.3% Tween 20 at room temperature. Slides were counterstained with DAPI. FISH signals were scored with a Zeiss epifluorescence microscope Zeiss Axio Imager-2 (Carl Zeiss Microimaging LLC, Thornwood, NY, USA) equipped with a DAPI/FITC/Rhodamine single band pass filters (Semrock, Rochester, NY) using 40-60× objectives.

RNA Expression

Expression profiling on Affymetrix GeneChip Human Exon 1.0 ST Arrays (Affymetrix, UK) was performed on CNS tissue obtained from 137 neurologically normal individuals at AROS Applied Biotechnology AS company laboratories (http://www.arosab.com/) (Trabzuni et al., 2011). Gene-level expression was calculated for C9ORF72 based on the median signal of probe 3202421. Date of array hybridization and brain bank were included as cofactors to eliminate batch effects.

For RT-PCR, RNA was extracted from brain tissue using Trizol (Invitrogen, Paisley, UK), and first-strand cDNA was synthesized using random primers using the Superscript II cDNA Synthesis Kit (Invitrogen). Real-time PCR analyses for C9ORF72 and GAPDH were performed using the ABI 7900 Sequence Detection System instrument and software (Applied Biosystems). Samples were amplified in quadruplicate in 10 μ l volumes using the Power SYBR-green master mix (Applied Biosystems), and 10 pM of each forward and reverse primer (see Supplemental Experimental Procedures online for primer sequences), using Applied Biosystems standard cycling conditions for real time PCR (initial denaturation at 95°C for 10 min, followed by 40 cycles of 95°C for 15 s, 60°C for 1 min).

Immunocytochemistry

Cells were fixed with ice-cold methanol for 2 min and blocked with 10% FBS for 30 min at 37°C. Primary antibody (anti-C9ORF72 antibody by Santa Cruz, sc-138763, 1:30) and secondary antibody (Alexa488-conjugated anti-rabbit antibody by Invitrogen, 1:200) were diluted in 5% FBS and incubated at 37°C for 3 hr or 30 min, respectively. The cells were then treated with 5 $\mu\text{g}/$ ml of Alexa633-conjugated wheat germ agglutinin (Invitrogen) in PBS for 10 min at room temperature (to detect cellular membranes), followed by incubation with 2 µg/ml propidium iodide (Invitrogen) in PBS for 3 min (to stain the nuclei). The cells were imaged with a TCS SP2 confocal microscope (Leica).

SUPPLEMENTAL INFORMATION

Supplemental Information includes three figures, Supplemental Experimental Procedures, and a list of the members of the ITALSGEN Consortium and can be found with this article online at doi:10.1016/j.neuron.2011.09.010.

ACKNOWLEDGMENTS

This work was supported in part by the Intramural Research Programs of the NIH, National Institute on Aging (Z01-AG000949-02), and NINDS. The work was also supported by the Packard Center for ALS Research at Hopkins (B.J.T.), the ALS Association (B.J.T., A.C.), Microsoft Research (B.J.T., P.J.T.), Ontario Research Fund (E.R.), Hersenstichting Nederland Fellowship project B08.03 and the Neuroscience Campus Amsterdam (J.S.-S.), Nuts Ohra Fonds (J.v.S.), Stichting Dioraphte (J.v.S. - Grant 09020300), the UK MND Association (H.M. - MNDA Grant 6057, J.H., R.W.O.), The Medical Research Council UK (J.H., S.P.B.), the Wellcome Trust (J.H.), the Helsinki University Central Hospital, the Finnish Academy (P.J.T.), the Finnish Medical Society Duodecim, Kuopio University, the Italian Health Ministry (Ricerca Sanitaria Finalizzata 2007, to A.C.), Fondazione Vialli e Mauro ONLUS (A.C.), Federazione Italiana Giuoco Calcio (A.C., M.S., B.J.T.) and Compagnia di San Paolo (A.C., G.R.), the European Community's Health Seventh Framework Programme (FP7/2007-2013) under grant agreements 259867 (A.C.) and 259867 (M.S., C.D.), Deutsche Forschungsgemeinschaft (M.S. - Grant SFB 581, TP4), the Muscular Dystrophy Association (M.B., J.W.), the Emory Woodruff Health Sciences Center (M.B., J.W.), EVO grants from Oulu University Hospital (A.M.R.) and the Finnish Medical Foundation (A.M.R.). DNA samples for this study were obtained in part from the NINDS repository at the Coriell Cell Repositories (http://www.coriell.org/), and the National Cell Repository for Alzheimer's Disease (http://ncrad.iu.edu). We thank the DNA extraction and storage facility of the National Institute for Health and Welfare/FIMM, Helsinki, Finland and Dr Tuomo Polvikoski, Institute for Ageing and Health, Campus for Ageing and Vitality, Newcastle University, Newcastle upon Tyne, UK for their help in extraction of DNA from ALS patients. We also thank Nayia Nicolaou for her assistance. J.R. is Director of the Packard Center for ALS Research at Hopkins, D. Harmer is an employee of Illumina, E.E.E. is on the scientific advisory board of Pacific Biosciences, and D. Heckerman is an employee of Microsoft Research. We thank the patients and research subjects who contributed samples for this study.

Accepted: September 14, 2011 Published online: September 21, 2011

Boxer, A.L., Mackenzie, I.R., Boeve, B.F., Baker, M., Seeley, W.W., Crook, R., Feldman, H., Hsiung, G.Y., Rutherford, N., Laluz, V., et al. (2011). Clinical, neuroimaging and neuropathological features of a new chromosome 9p-linked FTD-ALS family. J. Neurol. Neurosurg. Psychiatry 82, 196-203.

Cann, H.M., de Toma, C., Cazes, L., Legrand, M.F., Morel, V., Piouffre, L., Bodmer, J., Bodmer, W.F., Bonne-Tamir, B., Cambon-Thomsen, A., et al. (2002). A human genome diversity cell line panel. Science 296, 261-262

Chiò, A., Traynor, B.J., Lombardo, F., Fimognari, M., Calvo, A., Ghiglione, P., Mutani, R., and Restagno, G. (2008). Prevalence of SOD1 mutations in the Italian ALS population. Neurology 70, 533–537.

DeJesus-Hernandez, M., Mackenzie, I.R., Boeve, B.F., Boxer, A.L., Baker, M., Rutherford, N.J., Nicholson, A.M., Finch, N.A., Flynn, H., Adamson, J., et al. (2011). Expanded GGGGCC hexanucleotide repeat in noncoding region of C9ORF72 causes chromosome 9p-linked FTD and ALS. Neuron 72, in press. Published online September 21, 2011. 10.1016/j.neuron.2011.09.011.

Haaf, T., Sirugo, G., Kidd, K.K., and Ward, D.C. (1996). Chromosomal localization of long trinucleotide repeats in the human genome by fluorescence in situ hybridization. Nat. Genet. 12, 183-185.

Hirtz, D., Thurman, D.J., Gwinn-Hardy, K., Mohamed, M., Chaudhuri, A.R., and Zalutsky, R. (2007). How common are the "common" neurologic disorders? Neurology 68, 326-337.



Johnson, J.O., Mandrioli, J., Benatar, M., Abramzon, Y., Van Deerlin, V.M., Trojanowski, J.Q., Gibbs, J.R., Brunetti, M., Gronka, S., Wuu, J., et al; ITALSGEN Consortium. (2010). Exome sequencing reveals VCP mutations as a cause of familial ALS. Neuron 68, 857-864.

Kobayashi, H., Abe, K., Matsuura, T., Ikeda, Y., Hitomi, T., Akechi, Y., Habu, T., Liu, W., Okuda, H., and Koizumi, A. (2011). Expansion of intronic GGCCTG hexanucleotide repeat in NOP56 causes SCA36, a type of spinocerebellar ataxia accompanied by motor neuron involvement. Am. J. Hum. Genet. 89,

Kwiatkowski, T.J., Jr., Bosco, D.A., Leclerc, A.L., Tamrazian, E., Vanderburg, C.R., Russ, C., Davis, A., Gilchrist, J., Kasarskis, E.J., Munsat, T., et al. (2009). Mutations in the FUS/TLS gene on chromosome 16 cause familial amyotrophic lateral sclerosis. Science 323, 1205-1208.

Laaksovirta, H., Peuralinna, T., Schymick, J.C., Scholz, S.W., Lai, S.L., Myllykangas, L., Sulkava, R., Jansson, L., Hernandez, D.G., Gibbs, J.R., et al. (2010). Chromosome 9p21 in amyotrophic lateral sclerosis in Finland: a genome-wide association study. Lancet Neurol. 9, 978-985.

Lagier-Tourenne, C., Polymenidou, M., and Cleveland, D.W. (2010). TDP-43 and FUS/TLS: emerging roles in RNA processing and neurodegeneration. Hum. Mol. Genet. 19 (R1), R46-R64.

Li. H., and Durbin, R. (2009). Fast and accurate short read alignment with Burrows-Wheeler transform. Bioinformatics 25, 1754-1760.

Liehr, T., ed. (2009). Fluorescence In Situ Hybridization (FISH) Application Guide (Berlin: Springer-Verlag).

Lillo, P., and Hodges, J.R. (2009). Frontotemporal dementia and motor neurone disease: overlapping clinic-pathological disorders. J. Clin. Neurosci. 16. 1131-1135.

Lin, C.L., Bristol, L.A., Jin, L., Dykes-Hoberg, M., Crawford, T., Clawson, L., and Rothstein, J.D. (1998). Aberrant RNA processing in a neurodegenerative disease: the cause for absent EAAT2, a glutamate transporter, in amyotrophic lateral sclerosis. Neuron 20, 589-602.

Mackenzie, I.R., Rademakers, R., and Neumann, M. (2010). TDP-43 and FUS in amyotrophic lateral sclerosis and frontotemporal dementia. Lancet Neurol. 9. 995-1007.

Maruyama, H., Morino, H., Ito, H., Izumi, Y., Kato, H., Watanabe, Y., Kinoshita, Y., Kamada, M., Nodera, H., Suzuki, H., et al. (2010). Mutations of optineurin in amyotrophic lateral sclerosis. Nature 465, 223-226.

McKenna, A., Hanna, M., Banks, E., Sivachenko, A., Cibulskis, K., Kernytsky, A., Garimella, K., Altshuler, D., Gabriel, S., Dalv, M., and DePristo, M.A. (2010). The Genome Analysis Toolkit: a MapReduce framework for analyzing nextgeneration DNA sequencing data. Genome Res. 20, 1297–1303.

Mok, K., Traynor, B., Schymick, J., Tienari, P., Laaksovirta, H., Peuralinna, T., Myllykangas, L., Chio, A., Shatunov, A., Boeve, B., et al. (2011). The chromosome 9 ALS and FTD locus is probably derived from a single founder. Neurobiol. Aging, in press. Published online September 16, 2011. 10.1016/ j.neurobiolaging.2011.08.005.

Morita, M., Al-Chalabi, A., Andersen, P.M., Hosler, B., Sapp, P., Englund, E., Mitchell, J.E., Habgood, J.J., de Belleroche, J., Xi, J., et al. (2006). A locus on chromosome 9p confers susceptibility to ALS and frontotemporal dementia. Neurology 66, 839-844.

Neumann, M., Sampathu, D.M., Kwong, L.K., Truax, A.C., Micsenyi, M.C., Chou, T.T., Bruce, J., Schuck, T., Grossman, M., Clark, C.M., et al. (2006).

Ubiquitinated TDP-43 in frontotemporal lobar degeneration and amyotrophic lateral sclerosis. Science 314, 130-133.

Pearson, J.P., Williams, N.M., Majounie, E., Waite, A., Stott, J., Newsway, V., Murray, A., Hernandez, D., Guerreiro, R., Singleton, A.B., et al. (2011). Familial frontotemporal dementia with amyotrophic lateral sclerosis and a shared haplotype on chromosome 9p. J. Neurol. 258, 647-655.

Purcell, S., Neale, B., Todd-Brown, K., Thomas, L., Ferreira, M.A., Bender, D., Maller, J., Sklar, P., de Bakker, P.I., Daly, M.J., and Sham, P.C. (2007). PLINK: a tool set for whole-genome association and population-based linkage analyses. Am. J. Hum. Genet. 81, 559-575.

Rosen, D.R., Siddique, T., Patterson, D., Figlewicz, D.A., Sapp, P., Hentati, A., Donaldson, D., Goto, J., O'Regan, J.P., Deng, H.X., et al. (1993). Mutations in Cu/Zn superoxide dismutase gene are associated with familial amyotrophic lateral sclerosis. Nature 362, 59-62.

Rowland, L.P., and Shneider, N.A. (2001). Amyotrophic lateral sclerosis. N. Engl. J. Med. 344, 1688-1700.

Shatunov, A., Mok, K., Newhouse, S., Weale, M.E., Smith, B., Vance, C., Johnson, L., Veldink, J.H., van Es, M.A., van den Berg, L.H., et al. (2010). Chromosome 9p21 in sporadic amyotrophic lateral sclerosis in the UK and seven other countries: a genome-wide association study. Lancet Neurol. 9,

Sreedharan, J., Blair, I.P., Tripathi, V.B., Hu, X., Vance, C., Rogelj, B., Ackerley, S., Durnall, J.C., Williams, K.L., Buratti, E., et al. (2008). TDP-43 mutations in familial and sporadic amyotrophic lateral sclerosis. Science 319, 1668-1672.

Trabzuni, D., Ryten, M., Walker, R., Smith, C., Imran, S., Ramasamy, A., Weale, M.E., and Hardy, J. (2011). Quality control parameters on a large dataset of regionally-dissected human control brains for whole genome expression studies. J. Neurochem. Published online August 17, 2011. 10.1111/j.1471-4159.2011.07432.x.

Van Deerlin, V.M., Sleiman, P.M., Martinez-Lage, M., Chen-Plotkin, A., Wang, L.S., Graff-Radford, N.R., Dickson, D.W., Rademakers, R., Boeve, B.F., Grossman, M., et al. (2010). Common variants at 7p21 are associated with frontotemporal lobar degeneration with TDP-43 inclusions. Nat. Genet. 42, 234-239.

van Es, M.A., Veldink, J.H., Saris, C.G., Blauw, H.M., van Vught, P.W., Birve, A., Lemmens, R., Schelhaas, H.J., Groen, E.J., Huisman, M.H., et al. (2009). Genome-wide association study identifies 19p13.3 (UNC13A) and 9p21.2 as susceptibility loci for sporadic amyotrophic lateral sclerosis. Nat. Genet. 41, 1083-1087.

Vance, C., Al-Chalabi, A., Ruddy, D., Smith, B.N., Hu, X., Sreedharan, J., Siddique, T., Schelhaas, H.J., Kusters, B., Troost, D., et al. (2006), Familial amyotrophic lateral sclerosis with frontotemporal dementia is linked to a locus on chromosome 9p13.2-21.3. Brain 129, 868-876.

Vance, C., Rogelj, B., Hortobágyi, T., De Vos, K.J., Nishimura, A.L., Sreedharan, J., Hu, X., Smith, B., Ruddy, D., Wright, P., et al. (2009). Mutations in FUS, an RNA processing protein, cause familial amyotrophic lateral sclerosis type 6. Science 323, 1208-1211.

Warner, J.P., Barron, L.H., Goudie, D., Kelly, K., Dow, D., Fitzpatrick, D.R., and Brock, D.J. (1996). A general method for the detection of large CAG repeat expansions by fluorescent PCR. J. Med. Genet. 33, 1022-1026.

Wojciechowska, M., and Krzyzosiak, W.J. (2011). Cellular toxicity of expanded RNA repeats: focus on RNA foci. Hum. Mol. Genet. 20, 3811-3821.